Studying Fluid Characteristics Atop Surface Patterned Membranes via Particle Image Velocimetry

Didem Denizer[1,2], Ibrahim M. A. ElSherbiny[1,*], Mathias Ulbricht[2,3,4], and Stefan Panglisch[1,3,4,5]

DOI: 10.1002/cite.202100043

Surface patterning is a recent promising approach to promote performance of pressure-driven membranes in water treatment and desalination. Nevertheless, knowledge about foulant deposition mechanisms, especially at early stage of filtration, is still lacking. The applicability of particle imaging velocimetry to study fluid characteristics atop surface patterned thin-film composite membranes was investigated at different operating conditions. This work is an important first step toward reliable understanding of the impacts of topographical membrane surface modification on hydrodynamic conditions and foulant deposition mechanisms.

Keywords: Fluid characteristics, Hydrodynamic drag, Membrane fouling, Particle imaging velocimetry, Surface patterning

Received: April 25, 2021; *accepted:* June 17, 2021

1 Introduction

Surface patterned membranes are a versatile platform that can overcome limitations of feed spacers, as well as promote separation performance and antifouling propensity of pressure-driven membranes in water treatment and desalination applications [1, 2]. Membrane fouling and concentration polarization are among main obstacles that are challenging ultimate process efficiency, besides increasing energy demands and operation costs [3]. Simulations and lab-scale experiments have shown that manipulating membrane surface topography by introducing certain nano- or microstructures can potentially modify fluid characteristics and shear stress toward better antifouling behavior and less tendency for concentration polarization, without significantly increasing the pressure drop in the feed/retentate channel [4–7]. Nevertheless, such effects are critically influenced by the pattern design and dimensions, operating conditions, and characteristics of solute and/or foulants [8–10]. Moreover, reliable foulants deposition mechanisms on surface nano-/microstructures, especially in early filtration periods, are still lacking.

Surface patterned thin-film composite (TFC) membranes were recently introduced [7, 11]. Thanks to the enhanced membrane active surface area and outstandingly promoted membrane surface roughness, patterned membranes exhibited superior separation performance in both crossflow and dead-end experiments, compared to flat counterparts [7, 11, 12]. Additionally, alignment of surface microstructures with respect to feed flow direction was shown to influence the desalination performance [7, 11, 13]. Nevertheless, recent publications have emphasized that such effects are substantially influenced by several operating parameters (e.g., pattern design, crossflow velocity and size of solutes) [2, 4, 6, 7].

Particle imaging velocimetry (PIV) is a visual characterization technique, by which fluid characteristics in membrane-based feed channels can be quantitively investigated [14, 15]. In principle, fluorescent tracer particles ($< 50\,\mu m$) dispersed in the feed are pumped into a membrane fouling

[1]Didem Denizer, Dr. Ibrahim M. A. ElSherbiny, Prof. Dr.-Ing. Stefan Panglisch
ibrahim.elsherbiny@uni-due.de
University of Duisburg-Essen, Chair for Mechanical Process Engineering and Water Technology, Lotharstraße 1, 47057 Duisburg, Germany.

[2]Didem Denizer, Prof. Dr. Mathias Ulbricht
University of Duisburg-Essen, Chair for Technical Chemistry II, Universitätsstraße 7, 45141 Essen, Germany.

[3]Prof. Dr. Mathias Ulbricht, Prof. Dr.-Ing. Stefan Panglisch
Center for Water and Environmental Research (ZWU), Universitätsstraße 2, 45141 Essen, Germany.

[4]Prof. Dr. Mathias Ulbricht, Prof. Dr.-Ing. Stefan Panglisch
DGMT German Society of Membrane Technology, Geschäftsstelle ZWU, Universitätsstraße 2, 45141 Essen, Germany.

[5]Prof. Dr.-Ing. Stefan Panglisch
IWW Water Center, Moritzstraße 26, 45476 Mülheim an der Ruhr, Germany.

simulator. They are then illuminated by a laser with two light pulses separated by short time intervals that are set to track particles movement. A high-speed camera is recording the responses to two subsequent frames for laser light pulses that are analyzed in small interrogation areas, which enables identifying tracer particles displacement; thus, a velocity vector map can be produced. Some relevant examples are reported in literature [14–17].

In this work, the feasibility of vector velocity mapping and identification of fluid deceleration zones for the fluid atop surface patterned TFC membranes via 2D-PIV combined with a mini-plant reverse osmosis system (PIV-RO) was investigated. Micro-patterned TFC membranes were prepared by direct patterning of flat sheet TFC membranes via hot embossing micro-imprinting lithography. Toward more comprehensive insights, PIV measurements were performed for spacer-free and spacer-filled channels, at no permeation and permeation conditions, employing different crossflow velocities within laminar flow regime. Moreover, the impact of surface microstructures alignment with respect to feed flow direction on fluid characteristics was studied.

2 Materials and Methods

2.1 Membrane

A commercial spiral-wound module (FilmTec™ LC LE-4040) comprising PA TFC membrane was purchased from DuPont. According to the manufacturer, maximum operating pressure is 41 bar, and stabilized salt retention measured for 2000 ppm NaCl at 8.6 bar is 99.2 %. Flat sheet membrane samples were cut and stored in sodium metabisulfite solution (0.01 M). Prior to PIV experiments, membrane samples were rinsed in deionized (DI) water for 24 h. In case of patterned membrane samples, rinsing in 1:1 (v/v) ethanol-water solution for 1 h was done before immersing in DI water. Feed and permeate spacers were also cut from the module.

2.2 Direct Surface Partnering of Ready-to-Use PA TFC Membranes

The patterned PA TFC membranes were fabricated by hot embossing assisted micro-imprinting lithography [11] using a $35\times35\,cm^2$ brass mold in which a patterned area of $10\times10\,cm^2$ was prepared with an ultrashort pulse laser (GFH GmbH, Deggendorf, Germany). A symmetric line-and-groove pattern, comprising of parallel lines with a line width of 20 µm, a line-to-line width of 20 µm and a groove depth of 10 µm, was applied. The membrane with the PA layer facing the structured surface of the mold was placed on top of the metal mold and both were sandwiched between two thick steel plates. Patterning of PA TFC membranes was performed at 30 bar and 90 °C for 20 min. The fidelity of the produced patterned membranes was analyzed using an optical microscope (Motic, BA210 Digital). The performance of membranes was examined by measuring pure water permeability at a flux of $50\,L\,m^{-2}h^{-1}$ for 30 min and salt rejection using 2000 ppm NaCl employing a mini-plant testing unit (Convergence Industry B.V., Netherlands).

2.3 Characterization of Flow Characteristics via PIV

The flow characteristics, as vector-velocity mapping, atop surface-patterned vs. flat TFC membranes were characterized using 2D-PIV system (LaVision, Goettingen, Germany) combined with a mini-plant RO system (PIV-RO) [11]. The main components and configuration of the PIV-RO system are shown in Fig. 1. 2D-PIV system contains an Nd:YAG 532 nm laser and an high speed CCD camera (VC Imager Pro HS 500, LaVision, Germany); both connected to the DaVis software by LaVision. A custom designed stainless-steel flow cell with an optical window made of transparent acrylic glass (polymethylmethacrylate (PMMA), average visible light transmission > 92 %) was employed. The flow cell, also called membrane fouling simulator, has a permeate opening (to allow filtration mode), an active membrane area of $6.5\times26\,cm^2$, and a channel height of 0.1 cm (1000 µm). Prior to the measurement, a calibration was performed using single frame mode with an exposure time

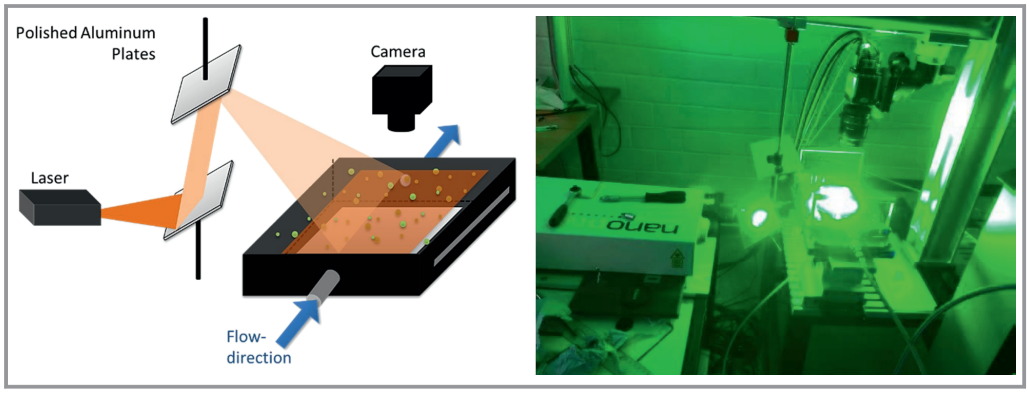

Figure 1. Schematic representation for the 2D-PIV system containing the flow cell with an acrylic glass window (left) and a photo of the PIV-RO system in operation (right).

of 5000 µs to correct distortions. Afterward, the camera was focused on the tracer particles. PMMA particles with a size range of 20–50 µm and modified with fluorescent Rhodamine B were purchased from LaVision (Germany) and employed as tracer particles. The PMMA particles had a density of 1.19 g cm^{-3}, i.e., close to water density, minimizing flow distortion or sedimentation due to different density. The feed dispersion was prepared by dispersing 0.05 g L^{-1} PMMA particles in DI water by means of an ultrasonic bath (Branson 5200) for 1 min. The measurement conditions were 65 % laser power and an imaging rate of 0.09 kHz at Δt = 8 µs using double frame rate. To maintain reliable measurements, the conditions were set in a way that each tracer particle should move about 5 pixels (~1.32 mm) per second. In this study, tracer particles were estimated to move ~6 pixels s^{-1} at a crossflow velocity of 0.15 m s^{-1}, and ~9 pixels s^{-1} at crossflow velocity of 0.22 cm s^{-1}. For every experiment, 20 images were taken for data processing and vector velocity mapping.

Fluid hydrodynamics were analyzed at different testing conditions. The surface patterned TFC membranes were installed with patterned grooves either parallel or perpendicular to the feed flow direction. PIV measurements were carried out at both permeation and no permeation conditions at feed pressure of 8 bar employing two average crossflow velocities of 0.15 m s^{-1} and 0.22 cm s^{-1}. Additionally, measurements were done with or without a feed spacer at 0.15 m s^{-1}.

It should be mentioned that the 2D-PIV setup had some limitations that influenced the measurement in this study. Lower vector velocities were recorded for all PIV measurements than the calculated mean crossflow velocities (in some cases the difference was an order of magnitude). This might be attributed to the nonuniform distribution of tracer particles in narrow flow channels (i.e., hydrodynamic classification of particles with respect to their size in laminar flow (Poiseuille flow) [18]). Another limitation is the possible overlapping of the intensities of reflected light from tracer particles moving in the lighted area at the same time but in various distances from the membrane surface. Accordingly, the general trends of velocity distribution profiles were considered in this study rather than the absolute vector velocity values.

3 Results and Discussion

3.1 Characterization of Surface Patterned PA TFC Membranes

The fidelity of the produced surface patterned PA TFC membranes was examined by optical microscopy [11] (cf. Fig. 2). A uniform pattern, with well-defined lines and grooves, was revealed. Moreover, pure water permeability and salt retention values for surface patterned membranes at different orientation were compared with those for flat TFC membranes. Surface patterned membranes exhibited a slightly lower pure water permeability (~3 L m^{-2}h^{-1}bar^{-1}) than flat membranes (4 L m^{-2}h^{-1}bar^{-1}), which might be related to compaction of membrane structure during the imprinting process. Nevertheless, salt retention values for surface patterned membranes were close to those for flat TFC membranes (cf. Fig. 2), emphasizing that the PA layer was intact and not damaged by the direct imprinting.

3.2 Fluid Characteristics Atop Surface Patterned PA TFC Membranes at No Permeation Conditions

The PIV experiments, and the results, were generally classified into two modes, no-permeation, and permeation conditions. Measurements at no permeation conditions were aimed at investigating the impacts of topographical membrane modification on hydrodynamic drag in the membrane proximity (i.e., simplified condition). In addition, measurements at permeation conditions were aimed at studying the impacts of surface patterning on fluid hydrodynamics in presence of permeation drag (i.e., promoting tracer particles interaction with the membrane surface).

Snapshots of velocity profiles for the fluid atop flat and surface patterned PA TFC membranes at no permeation condition and at different orientations, with or without using feed spacer are presented in Fig. 3. The measurements were performed at two average crossflow velocities 0.15 and 0.22 m s^{-1}, equivalent to *Re* numbers of 168 and 256, respectively (calculated for no feed spacer situation), i.e., laminar flow condition. Coloring indicators were fixed for all PIV images in this study; blue color refers to slow vector velocity while red color indicates high vector velocity.

Generally, velocity profiles for surface patterned vs flat membranes in spacer-free channels at no permeation condition did not show significant differences; overall low average velocity was measured for all membranes at different crossflow velocities. Nevertheless, flow field atop the flat TFC membranes seems to be slightly more irregular than

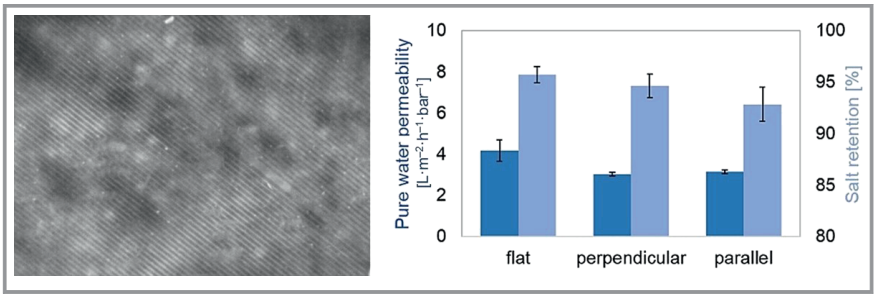

Figure 2. A microscope image for surface patterned PA TFC membrane (left), as well as pure water permeability and salt retention for surface patterned vs. flat PA TFC membranes (right).

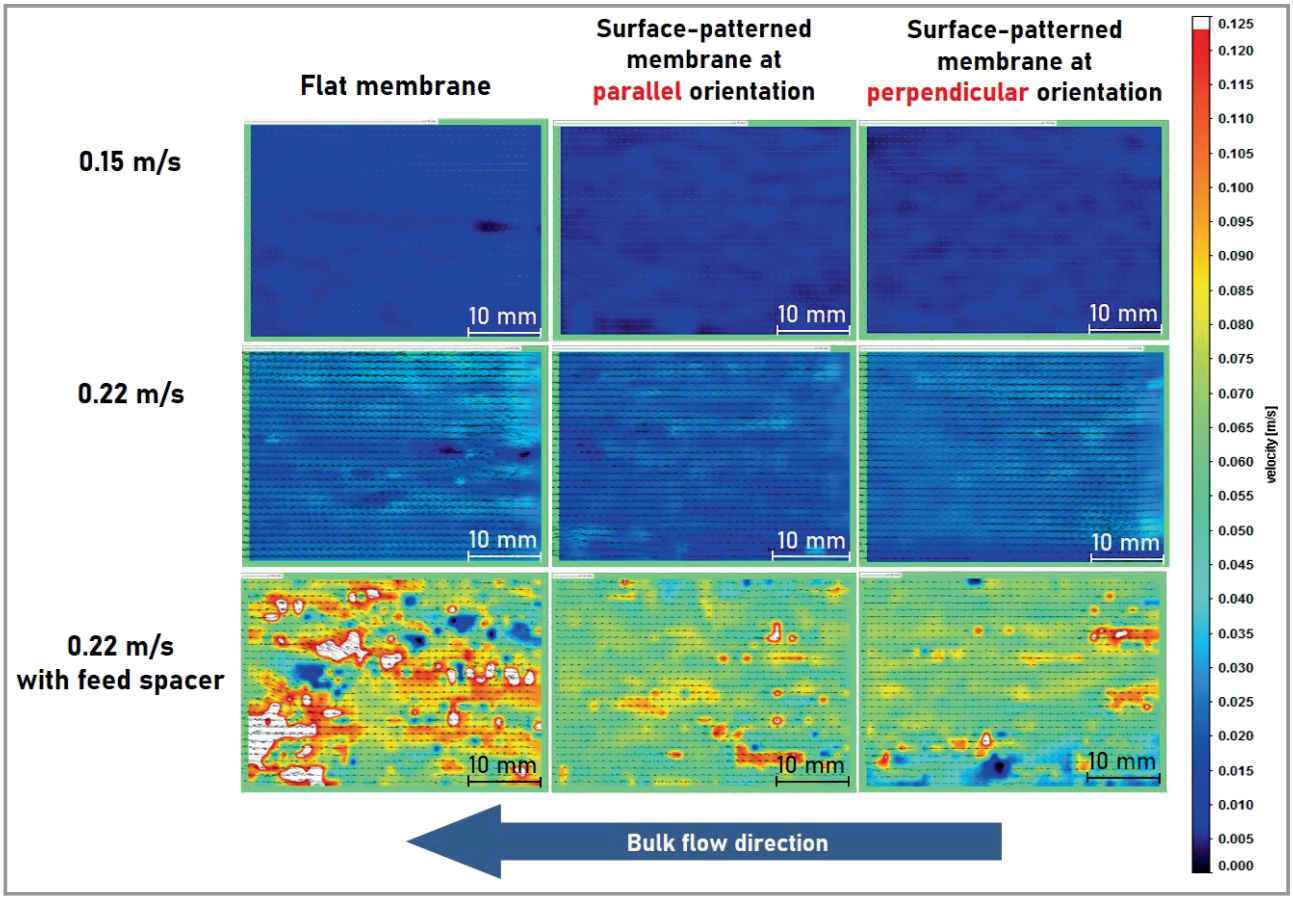

Figure 3. Snapshots of velocity profiles for the fluid atop surface patterned (at different orientation of the grooves relative to fluid flow) vs. flat TFC membranes, with or without using feed spacer, at no permeation condition and employing two average crossflow velocities, 0.15 m s^{-1} (*Re* = 168) and 0.22 m s^{-1} (*Re* = 256).

that in case of patterned membranes; a few elongated (dark colored) spots with a very low velocity can be seen at both crossflow velocities. In contrast, local velocity fluctuations were more regularly distributed in space for both patterned membranes at both crossflow velocities. However, at 0.22 m s^{-1}, surface-patterned membranes at perpendicular orientation exhibited a relatively higher (and more regular) average fluid velocity distribution than patterned membranes at parallel orientation. A regular and high average velocity distribution, and consequently hydrodynamic drag, is expected to result in high local velocity and thus high shear stress in the direct membrane vicinity. This will potentially lead to better fluid mixing, and therefore, lower membrane fouling and better membrane performance.

On the other hand, the PIV measurements in case of spacer-filled channels at average crossflow velocity of 0.15 m s^{-1} showed a different trend. The velocity profile for flat TFC membrane combined with feed spacer revealed a quite nonuniform flow velocity distribution, where one can see several spots with high vector velocities and other ones with low local velocities (i.e., fluid deceleration zones). Such deceleration zones among the turbulent bulk flow field, typical effect of feed spacers, might indicate formation of certain vortices that are regarded as potential fouling spots (i.e., vortex-induced shielding [10]). It is worth noticing that white colored areas in PIV images are indicating a higher vector velocity than the velocity scale set by the user. Nevertheless, if the velocity scale had been adjusted to include higher vector velocities, the differences between momentary velocity profiles in other testing conditions would have been difficult to detect.

Moreover, rather regular flow velocity distributions were seen in case of surface-patterned membrane at both orientations. However, the average velocity, over the entire observation area, atop patterned membranes at parallel orientation seems to be higher than that in case of perpendicular orientation (fluid deceleration spots were noticed at the edges, next to the channel walls). This observation might be explained by a possible trapping of (small) tracer particles between surface microstructures and feed spacer mesh because of entangled alignments. Furthermore, the average velocity, over the entire observation area, was revealed to be much higher for flat membranes than in case of patterned membranes. Such complex observation might be inter-

preted by a general deceleration (or partial trapping) of tracer particles between surface microstructures and feed spacer mesh, and/or overlapping of different momentary velocity profiles determined for multiple tracer particles layers at different distances from the membrane surface. Therefore, the results concerning fluid characteristics for spacer-filled channels measured by 2D-PIV should not be overestimated. To obtain more detailed information, e.g., bulk fluid velocity in the channel, not influenced by friction with the membrane surface, 3D stereo-PIV might be advantageous.

3.3 Fluid Characteristics Atop Surface Patterned PA TFC Membranes in Spacer-Free Channels at Permeation Conditions

In these experiments a pressure of 8 bar (maximum pressure allowed for acrylic glass in the flow cell) was applied and both permeate and retentate were recirculated back to the feed tank [11]. Fluid characteristics were investigated at different filtration intervals (0, 15, 30, 45 and 60 min) and constant average crossflow velocity of 0.15 m s^{-1} without using feed spacer. Snapshots of velocity profiles are presented in Fig. 4. It is worth noticing that intense blue colored spots located in the middle area of all images in Fig. 4 are referring to the permeation sink. This is where most of tracer particles were decelerated and/or deposited, due to the permeation drag, and consequently, the determined momentary vector velocity was the slowest. Nevertheless, different sizes of deceleration spots and local vector velocity ranges (indicated by different color intensity) might be related to either hydrodynamic conditions or measurement limitations (cf. Sect. 2.3). Again, white colored spots in some snapshots are indicating faster local vector velocity than the set velocity scale.

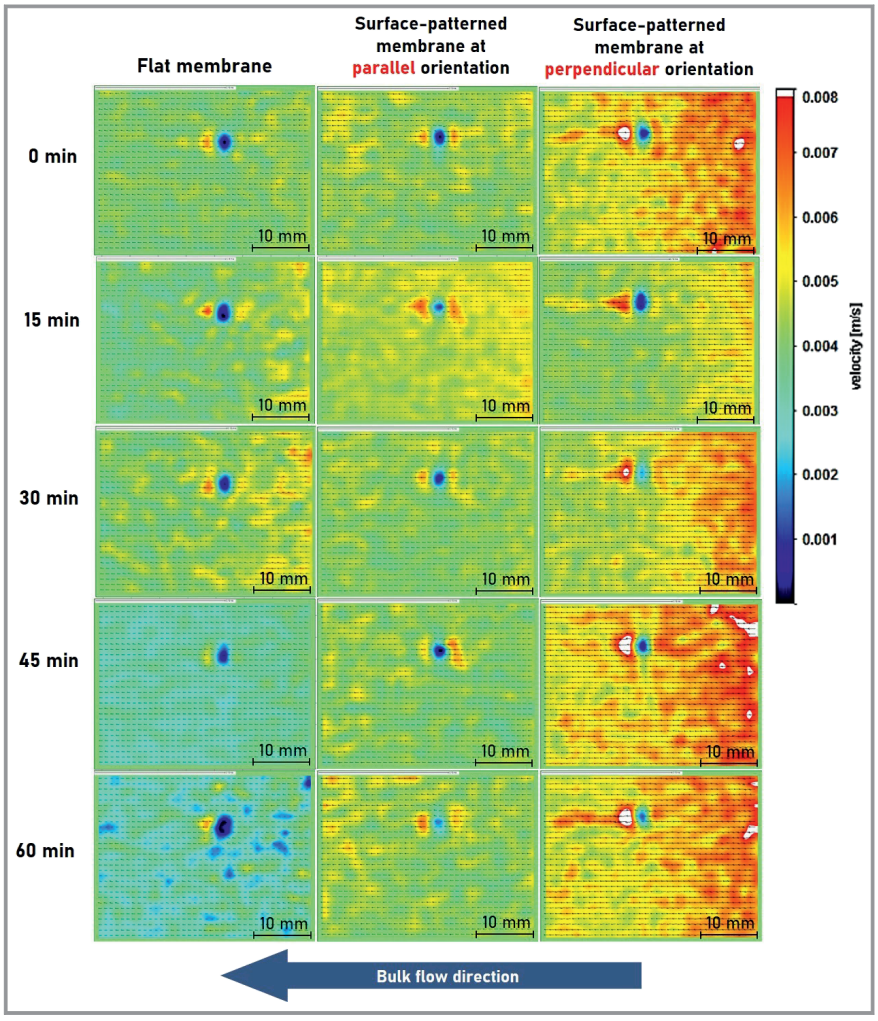

Figure 4. Snapshots of velocity profiles for the fluid atop surface patterned (at different orientation) vs. flat TFC membranes, without using feed spacer, at permeation condition, pressure of 8 bar, and crossflow velocity of 0.15 m s^{-1} (*Re* = 168). PIV images were recorded at different filtration intervals of 0, 15, 30, 45, and 60 min.

Generally, PIV measurements at permeation condition are expected to yield clearer observations concerning the impacts of topographical surface modification on hydrodynamic drag (i.e., fluid vector velocity distribution), and, consequently, wall shear stress and foulants accumulation in the membrane proximity. This is because, upon permeation, certain forces (e.g., permeation drag, attractive interaction) are acting to tracer particles forcing them toward the membrane surface, therefore more contact with membrane surface is implicated as well. In recent simulations, foulants accumulation on membranes surfaces, in spacer-free channels and at laminar regime, were emphasized to follow spatial patterns similar to that of fluid vector velocity distribution [8, 19, 20].

In case of flat membrane experiments, despite the fact that some spots of high vector velocities were noticed near the cell inlet in the snapshots recorded after 15 and 30 min, fluid deceleration zones were observed to form in streamwise direction during long filtration periods (up to 60 min). Such deceleration zones were found to significantly increase and regularly cover the observation area after 45- and 60-min intervals of starting the filtration experiment. The momentary vector velocity profile measured after 60 min was much slower, and the number of deceleration zones

was higher than those measured after 45 min. The pronounced fluid deceleration zones formed during long filtration periods indicate clearly low hydrodynamic drag, fluid mixing, and so, shear stress on membrane surface. This may potentially result in solutes and/or foulants accumulation, and hence, drastically influence the flat membranes performance.

On the other hand, substantially higher average vector velocities, resulting in stronger hydrodynamic drag, were measured for surface patterned membranes in both orientations. Surface patterned membrane at parallel orientation showed better trend (i.e., less tracer particles deceleration and higher average fluid velocity) compared to flat membrane. The highest and most regular vector velocity profile for surface patterned membrane at parallel orientation was noticed after 15 min; however, nonuniform fluid velocity distributions were found at later filtration periods (30, 45, and 60 min). In earlier study, surface microstructures at parallel orientation were assumed to homogenize bulk flow stream, induce surface mixing, and mitigate solute deposition at turbulent fluid conditions [7]. Nevertheless, here (i.e., PIV measurements in laminar condition), surface microstructures at parallel orientation seems to be not effective in promoting fluid mixing in the membrane proximity such that fluid deceleration zones were observed in the inlet and bottom regions of the observation area.

The highest average vector velocities and lowest tracer particles deceleration in PIV measurements at permeation condition were noticed in case of surface patterned membranes at perpendicular orientation. In addition, the local vector velocity was observed to gradually decrease in streamwise direction in all snapshots along the filtration period. However, vector velocity distributions measured at 0, 45, and 60 min looked very similar. Moreover, substantially low tracer particles deceleration revealed for surface patterned membranes at perpendicular orientation, compared to parallel orientation and flat membranes, might imply that surface microstructures at perpendicular orientation may induce fluid eddies that increase the wall shear stress in the membrane proximity and mitigate tracer particles deceleration and/or deposition, by shear-induced migration [10]. This is consistent with previously reported observations concerning lower fouling tendency for surface patterned ultrafiltration and nanofiltration membranes in spacer-free channels at perpendicular orientation [9, 21, 22]. Nevertheless, the impacts of surface patterning on fluid characteristics and fouling propensity are influenced by the size of tracer particles (or foulants, respectively), the average crossflow velocity (flow regime), as well as surface pattern design and dimensions. Therefore, further experiments are planned to better understand the effects of all influencing parameters and identify the most effective combination thereof for a particular membrane application.

4 Conclusions

The feasibility of studying fluid characteristics atop surface micro-patterned TFC membranes via a 2D-PIV system combined with a mini-plant RO testing unit was emphasized. The PIV-RO system was able to produce reliable snapshots of vector velocity profiles for the fluid atop surface patterned membranes in spacer-filled and spacer-free channels at different operating conditions (different crossflow velocities, with or without permeation). Generally, velocity profiles for surface patterned vs flat membranes in spacer-free channels at no permeation condition did not show significant differences; more uniform bulk flow stream was observed for surface patterned membranes. Latter observation was pronounced in case of PIV measurements in spacer-filled channels; the velocity profile for flat TFC membranes combined with feed spacer revealed a quite nonuniform flow velocity distribution, where deceleration zones were noticed among the turbulent bulk flow field.

In contrast, PIV measurements in spacer-free channels at permeation conditions showed substantially improved fluid characteristics for surface patterned membranes in both orientations of surface microstructures relative to bulk flow stream. Fluid deceleration spots atop flat TFC membranes were found to increase along filtration period; the slowest average vector velocities were measured after 60-min filtration interval. While substantially higher average vector velocities (that results in stronger hydrodynamic drag) were measured for surface patterned membranes in both orientations. The highest and most regular vector velocity profile for surface patterned membranes at parallel orientation was noticed after 15 min; however, rather nonuniform fluid velocity distributions were found at later filtration periods. Surface microstructures at parallel orientation seems to be not effective in promoting fluid mixing in the membrane proximity. Nevertheless, the best fluid characteristics (i.e., highest vector velocity (hydrodynamic drag) along with minimal tracer particles deceleration) were emphasized for surface patterned membranes in perpendicular orientation. The results of this work are consistent with reported conclusions from earlier studies, where either different membranes or different measurement methods had been used. This work is an important first step toward better understanding of foulants deposition mechanisms atop surface patterned TFC membranes at different alignments to the feed flow direction.

Authors acknowledge the support by Prof. Dr. Wojciech Kowalczyk, University of Duisburg-Essen, for offering an access to 2D-PIV system. Authors also acknowledge the support by Dr.-Ing. Ilka Gehrke, Fraunhofer UMSICHT institute, for offering an access to the hot embossing machine and for fabrication of metal molds. In addition, the support by M.Sc. Eliezer Kurnia, University of Duisburg-Essen, is highly appreciated. Open access funding enabled and organized by Projekt DEAL.

Abbreviation

PA	polyamide
PIV	particle imaging velocimetry
PMMA	polymethylmethacrylate
RO	reverse osmosis
TFC	thin-film composite

References

[1] O. Heinz, M. Aghajani, A. R. Greenberg, Y. Ding, *Curr. Opin. Chem. Eng.* **2018**, *20*, 1–12. DOI: https://doi.org/10.1016/j.coche.2018.01.008

[2] A. Malakian, S. M. Husson, *J. Membr. Sci.* **2020**, *10*, 445. DOI: https://doi.org/10.3390/membranes10120445

[3] N. Voutchkov, *Desalination* **2018**, *431*, 2–14. DOI: https://doi.org/10.1016/j.desal.2017.10.033

[4] Z. Zhou, B. Ling, I. Battiato, S. M. Husson, D. A. Ladner, *J. Membr. Sci.* **2021**, *617*, 118199. DOI: https://doi.org/10.1016/j.memsci.2020.118199

[5] Y. Ding, S. Maruf, M. Aghajani, A. R. Greenberg, *Sep. Sci. Technol.* **2017**, *52*, 240–257. DOI: https://doi.org/10.1080/01496395.2016.1201115

[6] W. Choi, C. Lee, D. Lee, Y. J. Won, G. W. Lee, M. G. Shin, B. Chun, T. S. Kim, H. D. Park, H. W. Jung, *J. Mater. Chem.* **2018**, *6*, 23034–23045. DOI: https://doi.org/10.1039/C8TA06125D

[7] I. M. A. ElSherbiny, A. S. G. Khalil, M. Ulbricht, *J. Membr. Sci.* **2017**, *529*, 11–22. DOI: https://doi.org/10.1016/j.memsci.2017.01.046

[8] Y.-J. Won, S.-Y. Jung, J.-H. Jang, J.-W. Lee, H.-R. Chae, D.-C. Choi, K. H. Ahn, C.-H. Lee, P.-K. Park, *J. Membr. Sci.* **2016**, *498*, 14–19. DOI: https://doi.org/10.1016/j.memsci.2015.09.058

[9] S. T. Weinman, S. M. Husson, *J. Membr. Sci.* **2016**, *513*, 146–154. DOI: https://doi.org/10.1016/j.memsci.2016.04.025

[10] S. Y. Jung, K. H. Ahn, *J. Membr. Sci.* **2019**, *572*, 309–319. DOI: https://doi.org/10.1016/j.memsci.2018.11.011

[11] D. Denizer, *Studying the fluid characteristics on top of micro-patterned membrane surfaces via Particle Image Velocimetry*, M. Sc. Thesis, University of Duisburg-Essen **2020**.

[12] I. M. A. ElSherbiny, A. S. G. Khalil, M. Ulbricht, *Membranes* **2019**, *9*, 67. DOI: https://doi.org/10.3390/membranes9060067

[13] V. Reimer, *Feasibility of different lithographic techniques and performance of resulting micro-patterned membranes*, M. Sc. Thesis, University of Duisburg-Essen **2018**.

[14] A. H. Haidari, S. G. J. Heijman, W. G. J. v.d. Meer, *Sep. Purif. Technol.* **2018**, *192*, 441–456. DOI: https://doi.org/10.1016/j.seppur.2017.10.042

[15] A. H. Haidari, S. G. J. Heijman, W. G. J. v.d. Meer, *Water Res.* **2016**, *106*, 232–241. DOI: https://doi.org/10.1016/j.watres.2016.10.012

[16] A. H. Haidari, S. G. J. Heijman, W. G. J. v.d. Meer, *Sep. Purif. Technol.* **2018**, *199*, 9–19. DOI: https://doi.org/10.1016/j.seppur.2018.01.022

[17] P. Willems, N. G. Deen, A. J. B. Kemperman, R. G. H. Lammertink, M. Wessling, M. v.S. Annaland, J. A. M. Kuipers, W. G. J. v.d. Meer, *J. Membr. Sci.* **2010**, *362*, 143–153. DOI: https://doi.org/10.1016/j.memsci.2010.06.029

[18] C. Sommer, S. Quint, P. Spang, T. Walther, M. Baßler, *WIT Trans. Eng. Sci.* **2014**, *82*, 265–277. DOI: https://doi.org/10.2495/AFM140231

[19] B. Ling, I. Battiato, *J. Fluid Mech.* **2019**, *862*, 753–780. DOI: https://doi.org/10.1017/jfm.2018.965

[20] S. Y. Jung, Y.-J. Won, J. H. Jang, J. H. Yoo, K. H. Ahn, C.-H. Lee, *Desalination* **2015**, *370*, 17–24. DOI: https://doi.org/10.1016/j.desal.2015.05.014

[21] R. J. Gohari, W. J. Lau, T. Matsuura, A. F. Ismail, *J. Membr. Sci.* **2013**, *446*, 326–331. DOI: https://doi.org/10.1016/j.memsci.2013.06.056

[22] S. H. Maruf, L. Wang, A. R. Greenberg, J. Pellegrino, Y. Ding, *J. Membr. Sci.* **2013**, *428*, 598–607. DOI: https://doi.org/10.1016/j.memsci.2012.10.059

DOI: 10.1002/cite.202100043
URN: urn:nbn:de:hbz:464-20210902-122031-3